Accurate complex modulation by the iterative spatial cross-modulation method

Yijun Qi (祁怡君)[1], Chenliang Chang (常琛亮)[2], and Jun Xia (夏 军)[1,*]

[1]*Joint International Research Laboratory of Information Display and Visualization, School of Electronic Science and Engineering, Southeast University, Nanjing 210096, China*

[2]*Key Laboratory for Opto-Electronic Technology of Jiangsu Province, Nanjing Normal University, Nanjing 210023, China*

**Corresponding author: xiajun@seu.edu.cn*

Received September 20, 2016; accepted December 6, 2016; posted online January 6, 2017

A method is proposed to realize accurate spatial complex modulation based on the spatial cross-modulation method (SCMM) via a phase-only spatial light modulator. The conventional SCMM cannot achieve high quality reconstruction, especially when the diffusion ratio is small. We propose an iterative algorithm in the calculation of a computer-generated hologram to implement accurate complex modulation. It enables us to generate a high quality reconstruction under a small diffusion ratio. The feasibility of the method is verified by both a numerical simulation and an optical experiment.

OCIS codes: 090.2870, 090.1760, 110.7348.
doi: 10.3788/COL201715.020901.

As we all know, holographic display can reconstruct the complex wave-front of an object. However, the development of a holographic display is hindered by low quality reconstruction, huge data process load, and lack of a complex modulation device[1]. Nowadays, the commercial optoelectronic devices can modulate the amplitude or its phase of the light wave independently, such as the phase-only spatial light modulators (SLMs) and the amplitude-only SLM[2,3]. Complex modulation[4], which permits the simultaneous modulation of amplitude and phase, is one of the methods for achieving high quality reconstruction. Meanwhile, complex modulations are utilized not only in display technology, but also for a variety of applications such as in pattern recognition[5], optical encryption[6], pulse shaping[7], beam shaping[8], optical tweezers[9,10], and optical communication[11].

Several methods have been proposed in regard to complex modulation. A well-known method for generating complex fields is by displaying an off-axis computer-generated hologram (CGH) on a phase-only SLM, in which the amplitude information is encoded as part of the phase information through interference with an off-axis reference plane wave[12,13]. Using this method, however, consumes energy of the incident plane wave, not only for the desired diffraction order, but also for unwanted diffraction orders, which limit the achievable diffraction efficiency. Another method for complex modulation is called the double-phase hologram (DPH)[14] applications based on the double-phase method have been proposed to contrive more desirable complex reconstruction[15,16]. Song *et al.* proposed an optical system for synthesizing double-phase complex CGHs using a phase-only SLM and a phase grating filter[17]. It should be noted that, although the diffraction efficiency is approximately equal to the off-axis method using a phase-only hologram[18], the above DPHs suffer loss of half of the spatial resolution in the output complex field. Mendoza-Yero *et al.* proposed a complex modulation method based on the double-phase method without the loss of spatial resolution in the output complex field[19]. In this method, the target complex object is obtained by spatially isolating a zeroth diffraction order.

Recently, Shibukawa *et al.* proposed a spatial cross-modulation method (SCMM), which uses a random phase diffuser and a phase-only SLM. The SCMM encodes a complex object as a scattered phase image by allowing the object to transmit through a random diffuser[18]. By virtue of this method, one can first get the reconstruction in an arbitrary space. Secondly, the speckle noise has been effectively suppressed due to complex modulation. Thirdly, in this method, there is no need to filter out other futile diffraction orders and pick up the first or zero order. Therefore, the resulting diffraction efficiency can be remarkably high. However, the SCMM has its defects. The main problem lies in that the quality of the reconstruction is proportional to the diffuser ratio. Here, the diffuser ratio is defined as the ratio of the pixel resolution of the diffuser and the target complex object. Sacrificing pixel resolution of the target complex object in an attempt for a higher diffuser ratio contributes to the improvement of inferior reconstruction. However, it renders this method undesirable in practical application compared with other conventional methods. To solve the above problem, we propose a method to improve the conventional SCMM. By virtue of using an iterative algorithm in generating a CGH, the quality of reconstruction is conspicuously improved in diverse diffuser ratios.

To begin with, the procedure of SCMM can be divided into two steps: the digital encoding step and the optical

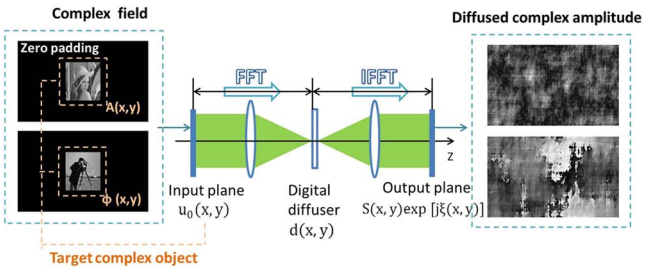

Fig. 1. Digital encoding step.

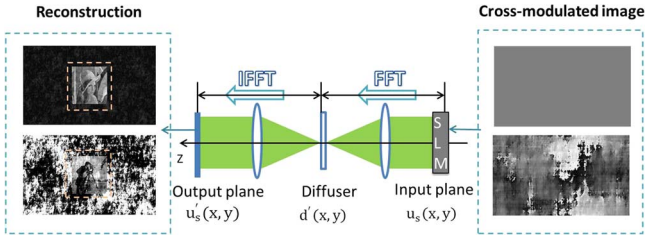

Fig. 2. Optical decoding step.

decoding step. As shown in Fig. 1, the digital encoding step is a 4f system. The desired complex amplitude in the input plane can be expressed as

$$u_0(x,y) = A(x,y)\exp[j\phi(x,y)]. \tag{1}$$

Calculated by the inverse fast Fourier transform (IFFT), the diffused complex amplitude in the output plane is expressed as

$$\begin{aligned} &S(x,y)\exp[j\xi(x,y)] \\ &\quad = \mathcal{F}^{-1}\{\mathcal{F}\{A(x,y)\exp[j\phi(x,y)]\}\exp[jh(x,y)]\}, \end{aligned} \tag{2.1}$$

where $\mathcal{F}\{\bullet\}$ denotes the operator of the two-dimensional Fourier transform. The spatial phase distribution of the digital random diffuser is denoted as $d(x,y) = \exp[jh(x,y)]$. It should be noted that, here only the diffused phase $\exp[j\xi(x,y)]$ is used in the optical decoding step, while the diffused amplitude $S(x,y)$ is discarded. Obviously, the nearer $S(x,y)$ approximates to being uniform, the smaller the effect of discarding it is. Here, Eq. (2.1) can be also written as

$$\begin{aligned} &S(x,y)\exp[j\xi(x,y)] \\ &\quad = A(x,y)\exp[j\phi(x,y)] * \mathcal{F}\{\exp[jh(x,y)]\}, \end{aligned} \tag{2.2}$$

where $\mathcal{F}\{\exp[jh(x,y)]\}$ is a two-dimensional impulse function, and it is also a stationary white noise[20]. The essence of this method lies in that the convolution of the target complex field with an impulse function can obtain a complex value, which has an approximately uniform amplitude distribution. One solution to enhance the amplitude uniformity is to decrease the pixel resolution of the target complex object to get a higher diffusion ratio. Consequently, we have the cross-modulated image as follows:

$$u_s(x,y) = \exp[j\xi(x,y)]. \tag{3}$$

After the preparation of the cross-modulated image, we get to the optical decoding step, which is shown in Fig. 2.

Only the phase of the complex hologram is loaded into the phase-only SLM. As shown in Fig. 2, the modulated light propagates through a 4f system with the diffuser at the frequency plane. Consequently, the reconstructed complex object is achieved at the output plane, which can be expressed as

$$\begin{aligned} u'_s(x,y) &= \mathcal{F}^{-1}\{\mathcal{F}\{\exp[j\xi(x,y)]\}\exp[-jh(x,y)]\} \\ &= A'(x,y)\exp[j\phi'(x,y)]. \end{aligned} \tag{4}$$

Here, the random phase diffuser $d'(x,y)$ should exactly be the conjugation of $d(x,y)$. In accordance with what we explained in the encoding step, the decoding step can be seen as the deconvolution of the cross-modulated image.

Although the complex modulation can be achieved by the SCMM, the reconstruction suffers low accuracy, especially under a small diffuser ratio. To improve the quality of reconstruction and achieve accurate complex modulation, an iterative algorithm is proposed in the digital encoding step, as shown in Fig. 3.

The iteration is demonstrated as follows:

(1) Create a complex field $k_0(x,y)$ as the initial value whose pixel resolution is exactly the same as the digital diffuser, $N_x \times N_y$ pixels. The target complex object $u_0(x,y)$ is placed in the center of the created complex field. It should be noted that we use a zero padding method to deal with the area around the target complex object[21].

(2) Employ an integrated conventional SCMM as mentioned above to get the output $k_n(x,y)$, which consists of the complex object $u'_{sn}(x,y) = A'(x,y)\exp[j\phi'(x,y)]$ and the noise pattern outside of the target complex object. The noise pattern area is the zero padding area in step (1), which now contains features of the original complex object.

(3) By substituting the original amplitude $A(x,y)$ and $\phi(x,y)$ phase for $A'(x,y)$ and $\phi'(x,y)$, respectively, and reserving the noise pattern, we get the updated kinoform $k_{n+1}(x,y)$.

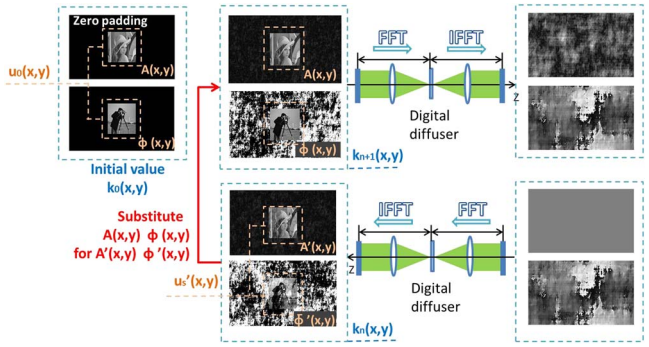

Fig. 3. Schematic of the proposed method.

(4) Evaluate the quality of the resultant complex object $u'_{sn}(x, y)$. If the error exceeds a threshold, redo steps (2) and (3) with $k_{n+1}(x, y)$ as the input or else the calculation stops.

The above iterative algorithm is based on the Gerchberg–Saxton (G–S) algorithm[22,23]. However, iteration is a reasonable optimized algorithm to effectively reduce the error between the desired complex object and the reconstruction, which ultimately achieves satisfied reconstruction. It should be noted that the difference between the proposed method and the iterative Fourier transform algorithm (IFTA) lies in that our proposed method gives a modified design of the iterative algorithm, in which both the desired amplitude and phase information are constraints.

The feasibility of the suggested method is verified by numerical simulations. The calculation is performed under conditions when (decoding process) the resolution of the created complex field is 1920×1080, the target complex object is 512×512 pixels, the wavelength used is 532 nm, (decoding process) the number of pixels of the phase-only SLM modeled in the simulation is 1920×1080, the modulation range of the SLM is $[0, 2\pi]$, and the number of gray levels of the SLM is 256. In addition, here we employ the famous "Lena" as the amplitude and the "Cameraman" as the phase.

We can see from Fig. 4, the reconstruction of the conventional SCMM suffers obvious artifacts. However, the artifacts are subsequently removed by our iteration algorithm. The output looks acceptable by iteration 5 and fine by iteration 9.

To evaluate the performance of complex modulation by the proposed method, we use the root-mean-square error (RMSE) as a metric, which is defined as

$$\mathrm{RMSE} = \sqrt{\frac{1}{M \times N}\sum_{ij}[x'(i,j) - X(i,j)]^2}, \qquad (5)$$

where $X(i,j)$ is the $X(i,j)_{\mathrm{th}}$ normalized pixel's ideal value of either the amplitude or phase of the target complex object, while $x'(i,j)$ is the normalized pixel's value of either the amplitude or phase of the reconstruction. The RMSE is used to measure the difference of the amplitude and phase between the target complex amplitude distributions and the reconstructed complex amplitude field.

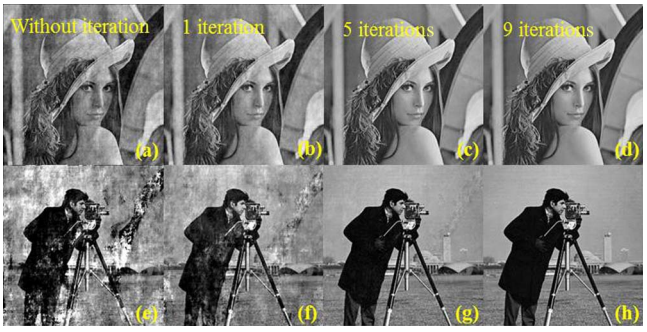

Fig. 4. Simulation results (a) and (e) from the conventional SCMM and (b) and (f), (c) and (g), and (d) and (h) the proposed method with different numbers of iterations using a random phase diffuser of the 256 gray level.

To further evaluate the performance of our proposed method, we compare it with the conventional SCMM, the off-axis method[13], and DPH method[19], respectively. The specifications of the phase-only SLM modeled in the simulations are as follows: the number of pixels is 1920×1080, the pixel pitch is 8 μm, the modulation range is $[0, 2\pi]$, and the number of gray levels is 256. Besides, the common parameters in the simulations are listed as follows: the wave length is 532 nm, and the resolution of the target complex object is 512×512. In the conventional SCMM and the proposed method, we employ the same 256 gray-level random phase diffuser whose resolution is 1920×1080 (the diffusion ratio is 7.9). In the off-axis method, the incident angle of the off-axis reference plane wave interfering with the object is 1.1°. The off-axis method and the DPH method both involve a filter at the Fourier plane of the 4f optical system. The size of the square aperture used in the simulation of the off-axis method and the DPH method is optimized to obtain the lowest RMSE. The simulation results are shown in Fig. 5 and Table 1.

We can see that the reconstruction of proposed method in Figs. 5(a) and 5(e) is better than the reconstruction of the conventional SCMM without iteration that is shown in Figs. 5(b) and 5(f), the off-axis method in

Fig. 5. Reconstructed amplitude and phase. (a) and (e) by the proposed method at 50 times iterations. (b) and (f) by the conventional SCMM. (c) and (g) by the off-axis method. (d) and (h) by the DPH method.

Table 1. RMSE Comparison Among Our Method at 50 Times Iterations, Conventional SCMM[18], Off-axis Method[13], and DPH Method[19]

	Proposed method	Conventional SCMM	Off-axis method	DPH method
Amplitude	0.0017	0.0989	0.0546	0.0443
Phase	0.0088	0.3454	0.3900	0.1926

Figs. 5(c) and 5(g), and the DPH method in Figs. 5(d) and 5(h). The results of the conventional SCMM without iteration in Figs. 5(b) and 5(f) and off-axis method in Figs. 5(c) and 5(g) suffer obvious artifacts, while the results of the DPH method in Figs. 5(d) and 5(h) suffer slight speckle noise. In order to further compare the results quantitatively, Table 1 presents us the RMSEs of the reconstructions. It shows that the RMSE of the amplitude of the proposed method is smaller than 0.0017 after 50 iterations, and the RMSE of the phase is smaller than 0.0088 after 50 iterations. Figure 5 and Table 1 demonstrate that with the help of the proposed iterative algorithm, the reconstruction, which was worse than the other two complex modulation methods under this diffusion ratio, is conspicuously improved. It should be noted that the conventional SCMM without iteration is worse under this diffusion ratio, and it cannot be improved by using the G–S or IFTA algorithms with only one constraint.

To demonstrate that the conventional SCMM cannot achieve high quality reconstruction especially when the pixel resolution of the reconstruction is close to the diffusion pattern (that means the diffusion ratio is close to 1) and the proposed method can effectively improve the reconstruction, we further performed another experiment. The specifications of the phase-only SLM modeled in the simulations are as follow: the number of pixels is 1920×1080, the modulation range is $[0, 2\pi]$, and the number of gray levels is 256. It should be noted that the pixel resolution of the target complex objects are 768×768 (diffusion ratio is 3.5), 512×512 (7.9), and 256×256 (31.6), respectively.

Figure 6 shows the reconstruction of the amplitude and phase whose resolution is 768×768 (diffusion ratio is 3.5), 512×512 (7.9), and 256×256 (31.6), respectively, by the conventional SCMM, and the proposed method with the same diffuser when the complex field is 1920×1080. Compared with Figs. 6(a) and 6(b), 6(e) and 6(f), and 6(i) and 6(j), the reconstructions of the smaller complex objects (higher diffusion ration) are better than those of larger objects, although they still suffer artifacts. This trait agrees well with the above discussion of the principle. Figure 6 and Table 2 show that by iteration 50, the algorithm converging and the reconstruction of three different complex objects with pixel resolutions 768×768 (diffusion ratio is 3.5), 512×512 (7.9), and 256×256 (31.6), respectively, are improved without striking artifacts and speckle noises. By virtue of the proposed method, we can get high quality reconstruction when the diffusion ratio is small.

Fig. 6. Created complex field $k_0(x, y)$ 1920×1080, reconstruction of the amplitude and phase at (a) and (b) 768×768, (e) and (f) 512×512, (i) and (j) 256×256 by the conventional SCMM. Reconstruction of the amplitude and phase at (c) and (d) 768×768, (g) and (h) 512×512, (k) and (l) 256×256 by the proposed method at 50 times iterations.

Figure 7(a) shows the RMSE curves of the reconstructed amplitude image at various diffusion ratios, and Fig. 7(b) shows the RMSE curves of the reconstructed phase image at various diffusion ratios. As we can see from Fig. 7, all of the RMSE curves converge after certain numbers of iteration. For diffusion ratios that are larger than 3.5, the RMSEs decrease rapidly during the first 15 iterations, and then reach a plateau at a level smaller than 0.02 for the amplitude and 0.06 for the phase. For a diffusion ratio smaller than 2, the RMSEs decrease, but the curves reach a plateau at a level of 0.12 for the amplitude and 0.36 for the phase. So, when the diffusion ratio is higher than about 3.5, the proposed method can more effectively improve the quality of the reconstruction.

The optical setup of the single lens system in our experiment is shown in Fig. 8. We use a 532 nm laser to illuminate the phase-only SLM1 (Holoeye Pluto, resolution:

Table 2. RMSE Comparison Between Our Method at 50 Times Iterations and the Conventional SCMM[18] for Different Resolutions of Reconstructed Amplitudes

	Conventional SCMM		Proposed method	
	amplitude	phase	amplitude	phase
768×768	0.1283	0.3646	0.0011	0.0039
512×512	0.0989	0.3454	0.0017	0.0088
256×256	0.0346	0.2421	0.0016	0.0057

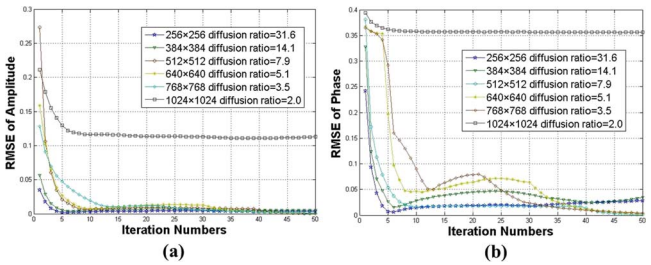

Fig. 7. (a) RMSE curves of the reconstructed amplitude image at various diffusion ratios. (b) The RMSE curves of the reconstructed phase image at various diffusion ratios.

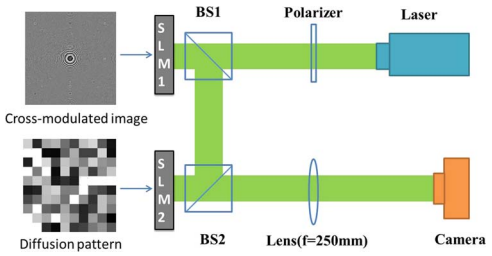

Fig. 8. Schematic setup used to measure the amplitude of a complex object.

1920×1080, pixel pitch: 8 μm). The input plane of this optical system coincides with the SLM1 plane. Here, the phase-only SLM2 (Reallight, RL-SLM-R2, resolution: 1280×1024, pixel pitch: 12.3 μm) functions as the diffuser at the frequency plane. The created complex field $k_0(x, y)$ is 1000×1000, and the reconstructed complex object is 768×768. The intensity of the complex object is recorded directly by the CMOS of the camera (Nikon D3100) at the focal plane of the lens. It should be noted that the lens between SLM1 and SML2 is removed by compensating two quadratic phase factors during the calculation of the hologram. Propagation from the input plane to the diffuser plane under distance z can be analyzed by the Fresnel diffraction, and the relation between the input plane and the output plane is given by

$$O(x_o, y_o) = \mathcal{F}^{-1}\left\{\mathcal{F}\left[I'(x_i, y_i) \cdot \exp\left[\frac{i\pi(x_i^2 + y_i^2)}{\lambda z}\right]\right] \cdot \exp\left[\frac{i\pi(x_d^2 + y_d^2)}{\lambda z}\right] \cdot d'(x_d, y_d)\right\} = \mathcal{F}^{-1}\{\mathcal{F}[I(x_i, y_i)] \cdot d(x_d, y_d)\}. \quad (6)$$

Before the experiment, pre-alignment between the SLM1 and SLM2 is a significant procedure because the reconstructed signal is achieved via overlap of the fields at the frequency plane pixel by pixel. Here, we employ an alignment strategy of the 4f system to achieve better alignment[20].

The results using the conventional SCMM and the proposed method by iteration 20 with the same diffusion pattern are shown in the Fig. 9. Figures 9(a) and 9(c) are the numerical results of amplitude of the conventional SCMM and the proposed method by iteration 20. Figures 9(b) and 9(d) are the optical results of the intensity of the conventional SCMM and the proposed method by iteration 20 shifted away from the zero order beam. The random phase diffuser pattern used here is 10×10 data pixels, as shown in Fig. 8. Each data pixel consists of 100×100 pixels of the SLM. As we can see from Fig. 9, the optical results are consistent with the numerical results. The speckle noise is suppressed due to complex modulation. The quality of reconstruction is improved by the proposed method in a more concise system.

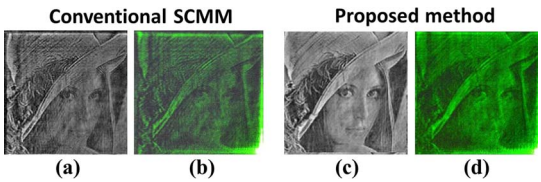

Fig. 9. (a) and (c) Numerical results of the amplitude of the conventional SCMM and the proposed method by iteration 20. (b) and (d) Optical results of the intensity of the conventional SCMM and the proposed method by iteration 20. The phase of the reconstructed object is zero.

In this Letter, an iterative method to improve the quality of reconstruction using the SCMM is presented. Our work contributes to the further development of the SCMM by breaking through the limit of the diffusion ratio and remarkably improving the quality of reconstruction.

This work was supported by the National "973" Program of China (No. 2013CB328803) and the National "863" Program of China (Nos. 2015AA016301 and 2013AA013904).

References

1. Y. Zhang, J. Liu, X. Li, and Y. Wang, Chin. Opt. Lett. **14**, 030901 (2016).
2. X. Gaolei, L. Juan, L. Xin, J. Jia, Z. Zhao, H. Bin, and W. Yongtian, Opt. Express **22**, 18473 (2014).
3. X. Ma, J. Liu, Z. Zhang, X. Li, J. Jia, B. Hu, and Y. Wang, Chin. Opt. Lett. **13**, 010901 (2015).
4. J. Alexander, M. Christian, S. Andreas, B. Stefan, and R. M. Monika, Opt. Express **16**, 2597 (2008).
5. J. Campos, A. Márquez, M. J. Yzuel, J. A. Davis, D. M. Cottrell, and I. Moreno, Appl. Opt. **39**, 5965 (2000).
6. P. C. Mogensen and J. Glückstad, Opt. Lett. **25**, 566 (2000).
7. A. M. Weiner, J. P. Heritage, and E. M. Kirschner, J. Opt. Soc. Am. B **5**, 1563 (1988).
8. S. Tao and W. Yu, Opt. Express **23**, 1052 (2015).
9. J. Alexander, M. Christian, S. Andreas, B. Stefan, and R. M. Monika, Opt. Express **16**, 4479 (2008).
10. J. Wang, Photon. Res. **4**, B14 (2016).
11. J. Wei, L. Geng, D. G. Cunningham, R. V. Penty, and I. White, in *Proceedings of OFC/NFOEC13* (2013), paper OW4A.5.
12. J. A. Davis, D. M. Cottrell, J. Campos, M. J. Yzuel, and I. Moreno, Appl. Opt. **38**, 5004 (1999).
13. X. Li, J. Liu, J. Jia, Y. Pan, and Y. Wang, Opt. Express **21**, 20577 (2013).
14. C. Hsueh and A. Sawchuk, Appl. Opt. **17**, 3874 (1978).
15. V. Arrizón, Opt. Lett. **28**, 1359 (2003).
16. V. Arrizón, Opt. Lett. **28**, 2521 (2003).
17. H. Song, G. Sung, S. Choi, K. Won, H.-S. Lee, and H. Kim, Opt. Express **20**, 29844 (2012).
18. A. Shibukawa, A. Okamoto, M. Takabayashi, and A. Tomita, Opt. Express **22**, 3968 (2014).
19. O. Mendoza-Yero, G. Mínguez-Vega, and J. Lancis, Opt. Lett. **39**, 1740 (2014).
20. P. Refregier and B. Javidi, Opt. Lett. **20**, 767 (1995).
21. A. Georgiou, J. Christmas, N. Collings, J. Moore, and W. Crossland, J. Opt. A: Pure Appl. Opt. **10**, 035302 (2008).
22. R. W. Gerchberg, Optik **35**, 237 (1972).
23. C.-Y. Chen, H.-T. Chang, T.-J. Chang, and C.-H. Chuang, Chin. Opt. Lett. **13**, 110901 (2015).